한국항해항만학회지 제40권 제5호
J. Navig. Port Res. Vol. 40, No. 5 : 231-239, October 2016 (ISSN:1598-5725(Print)/ISSN:2093-8470(Online))
DOI : http://dx.doi.org/10.5394/KINPR.2016.40.5.231

Development of 6-DOF Equations of Motion for a Planning Boat Based on the Results of Sea Trial Tests

Myung-Jun Jeon · Dong-Hyun Lee* · † Hyeon-Kyu Yoon*

* *Graduate school of Changwon National University, Gyeongnam, 51140, Korea*
† *Associate Professor of Changwon National University, Gyeongnam, 51140, Korea*

Abstract : *In general, the attitude of a high-speed planning boat changes following a speed change. Since the hydrodynamic forces acting on a ship differ according to the change of its underwater shape, it is difficult to estimate its hydrodynamic force compared to that of a large commercial ship. In this paper, 6 Degrees Of Freedom (DOF) equations of motion that express the maneuvering motion of a planning boat are modeled by analyzing its motion characteristics based on various sea trial tests. Finally, a maneuvering simulation is carried out and a validation of the equations of motion is confirmed with the results of sea trial tests.*

Key words : *Planning boat, 6-DOF equations of motion, Maneuvering, Modeling, Sea trial*

1. Introduction

As domestic enjoyment of marine leisure sports has expanded and become more diverse, 30 marinas have been installed and the number of leisure boats has increased 2.6 times during the past 5 years. In addition, government agencies associated with the marina industry have announced that the expansion has created 8,000 new jobs and brought in 55,000 million dollars; also, the number of boats will double by 2017. Fig.1 shows the expected effect of the expansion of the marina industry (Promotion Plan, 2014). A ripple effect has also led to an increase in the number of educational institutions for boating licenses.

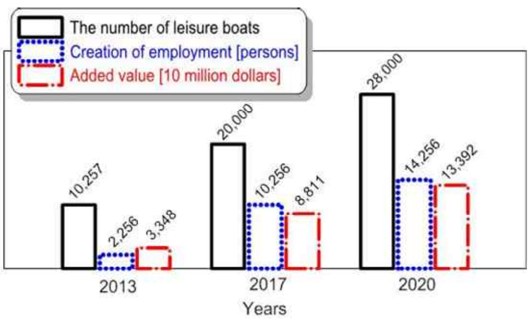

Fig. 1 Expected effects from promotion of the marina industry

The number of people who wish to operate leisure boats has increased, but the number of educational institutions and leisure boats is insufficient for their needs. For this reason, ship handling simulators, which emulate the motion of a real boat, are being developed. Kang and Yoon(2013) conducted a study on the conceptual design of a leisure boat handling simulator. Fig. 2 shows the sample ship handling simulator. It is generally composed of two parts. One is a fixed part including a motion solver unit, a main control unit and a graphic display unit. The other is a moving part which includes a dashboard unit and a motion base unit.

Fig. 2 Ship handling simulator

Yoon et al.(2007a) developed a simplified horizontal maneuvering model of an RIB-type target ship and verified

† Corresponding author : hkyoon@changwon.ac.kr 055)213-3683
* jmj5390@daum.net 055)213-2930
* dhzzang3@gmail.com 055)213-2930

Note) This paper was presented on the subject of "Development of 6-DOF Equations of Motion for a Planning Boat based on the Results of Sea Trial tests" in 16th Asian Conference on Maritime System and Safety Research proceeding(Korea Maritime and Ocean University, 18th Aug-19th Aug, 2016, pp.159-166)

the model by comparing it with the results of a sea trial. Yoon et al.(2007b) estimated system model of roll hydrodynamic moment used a system identification method and a free-running model test and verified the model by comparing it with a free-running model test. Kim et al.(2010) carried out an analytical approach with a simple maneuvering model to develop a mathematical model for a simulator based on Yoon et al's(2007a) previous model. In addition, Kim et al.(2010) suggested the speed and turning model, which is described by a 1^{st} order differential equation with respect to speed and rate of turns. Yeo and Rhee(2005) suggested hydrodynamic coefficients which are sensitive to specific maneuvering motions using sensitivity analysis.

When anticipating the motion of a planning boat, the hydrodynamic force and moment are taken into account according to its attitude. In other words, the hydrodynamic force and moment are function of its speed(Lewandowski, 2002). Also, the lift at the bottom side of a ship arises when a planning boat runs in calm water. So, the vertical position of the body and pitch angle change depending on time. The changes in pitch angle vary when the boat goes straight versus when it moves in a rotational manner. Therefore, the dynamic model should be in the form of a 6 DOF mathematical model.

In this paper, we defined the structure of a mathematical model and identified the parameters composing model structures after conducting an analysis of sea trial results. And, the methods for identifying model parameters are proposed. The corrected mathematical models were verified by carrying out numerical simulations and comparing the results of simulations and sea trials. The feasibility of the mathematical models for emulating motion similar to a real boat's motions was confirmed as the models for the ship handling simulator

2. Sea trial

2.1 Target boat and test equipment

The target boat is an 18 ft motor boat, which is shown in Fig. 3. The hull is made up of FRP (Fiber Reinforced Plastics) and the maneuvering motion of the boat is conducted by the changes of outboard motor angles. The principal dimensions of the boat are listed in Table 1.

Fig. 3 Actual feature of the 18 ft motor boat

Table 1 Principal dimensions of the motor boat

Item (unit)	Value
Length (m)	5.45
Breadth (m)	2.00
Depth (m)	0.98
Draft (m)	0.44
Volume (m^3)	0.96
Maximum thruster angle (°)	35.0
Outboard motor	MERCURY 115 hp

The sensor for measuring ship motion variables is NAV440CA-200, which is shown in Fig. 4 (MEMSIC). This sensor is able to measure angular rate and acceleration with inertial sensors and trajectories using a GPS receiver. In order to develop a realistic ship handling simulator, noise from the boat's engine and the display on the driver's seat should be properly modeled separately from the ship's dynamics. Therefore, other equipments were applied to the sea trial, as listed in Table 2.

Fig. 4 Inertia Measurement Unit (IMU) sensor

Table 2 Extra equipment, including the IMU sensor

Model name	Measurement or recording variables
NAV440CA-200	Ship motions
SONY ICD-UX560F	Engine noise
GoPro HERO4 Black	Display on driver's seat
SPI TRONIC PRO3600	An angle of inclination

2.2 Scenario and correction methods

In order to develop a 6 DOF dynamic model using the results of a sea trial, the scenario for the sea trial must be suitable for obtaining motion variables in accordance with each test condition. The scenario used for the sea trial is listed in Table 3. The notation s.s. written in the description indicates “steady state.” Straight running tests were carried out to analyze the attitude of the target boat according to ship speed. Also, turning tests were needed to investigate yaw rate and roll angle depending on the changes in outboard motor angle and ship speed. The correlation between yaw rate and sway velocity can be estimated by analyzing the result of the zig zag test as well as that of the turning test.

Table 3 Scenario for the sea trial

Code	Test	Description
ST01	Straight	- Low speed - Steady forward velocity - Measure for 10s at s.s.
ST02	Straight	- Middle speed - Steady forward velocity - Measure for 10s at s.s.
ST03	Straight	- High speed - Steady forward velocity - Measure for 10s at s.s.
TR01	Turning	- Low speed - Full motor angle at s.s. - Record 720° turning circle
TR02	Turning	- Middle speed - Full motor angle at s.s. - Record 720° turning circle
ZZ01	Zig Zag	- Middle speed - Full motor angle at s.s. - Record 3 periods of heading angle

Fig. 5 Actual features of the sea trial taken from an earth-fixed camera and a ship-fixed camera

Since a GPS receiver was not installed on the center of the ship’s body, the trajectory and velocity measured by the GPS had to be transformed to ones that corresponded to the center of the body-fixed coordinate. Fig. 6 shows the position of the GPS receiver at the time of the sea trial. The distance between the origin of the boat and the position of the GPS receiver was 2.5 m in the direction of the longitudinal axis. So, the velocity vectors which need to be corrected are defined in Eq. (1). In addition to the velocity vectors, the trajectories of the boat could differ owing to the difference between the position of the GPS receiver and the ship’s origin. The correction formula for that trajectory is defined in Eq. (2). The displacement vectors in Eq. (2) were obtained by converting longitude and latitude to distance in meters.

$$\underline{u}_0 = \underline{u} - \underline{\omega} \times \underline{r}_{GPS} \tag{1}$$

$$\underline{R}_0 = \underline{R} - C_b^n \underline{r}_{GPS} \tag{2}$$

where,

$\underline{u}_0$ Velocity vector at the origin

$\underline{u}$ Velocity vector at the GPS receiver

$\underline{\omega}$ Angular rate vector at the GPS receiver

$\underline{r}_{GPS}$ Position vector of the GPS receiver w.r.t. the body-fixed coordinate

$\underline{R}_0$ Position vector of the origin of the boat w.r.t. the earth-fixed coordinate

$\underline{R}$ Position vector of the GPS receiver w.r.t. the earth-fixed coordinate

C_b^n Linear transformation matrix from the body-fixed coordinate to the earth-fixed one(Fossen, 1994)

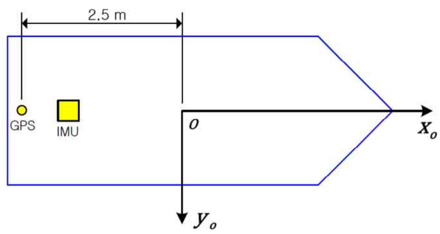

Fig. 6 Description of GPS position

2.3 Correlation analysis

Before defining the structures of the mathematical model, correlation analysis regarding each motion variable should be necessary to investigate which parameters in the model must mainly be considered.

As shown in Fig. 7, the sample correlation coefficients of velocities v and r appear to take on the greatest values, which means that there are strong coupling effects between sway and yaw. Also, the correlation between pitch rate q and yaw rate r differs in the turning test and the zig zag test. In other words, the model parameter expressing the relationship between pitch rate and yaw rate is necessary to properly determine the model structure. The reason why the sample correlation coefficient between surge velocity u and sway velocity v appears to be high is because they share a similar convergence time when the ship turns. Contrary to the turning test, the correlation between u and v is low because surge acceleration and sway acceleration are more dominant in the zig zag test.

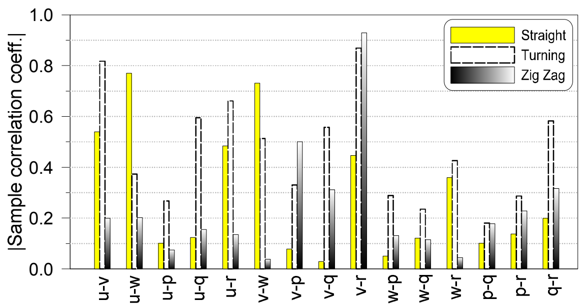

Fig. 7 Absolute value of sample correlation coefficients between velocity vectors during each test

3. Dynamic modeling

3.1 Coordinate systems and equations of motion

6 DOF equations of motion are defined in a body-fixed coordinate $(o - x_0 y_0 z_0)$, which is shown in Fig. 8. Commonly, positive directions of x_0, y_0 and z_0 are defined as the directions of forward, starboard, and downward. An Earth-fixed coordinate $(O - xyz)$ is used to express a ship's trajectory and attitude. 6 DOF equations of motion are expressed using Newton's 2^{nd} law. Environmental effects such as wind, wave, and current are not included in the external forces and moments in this paper.

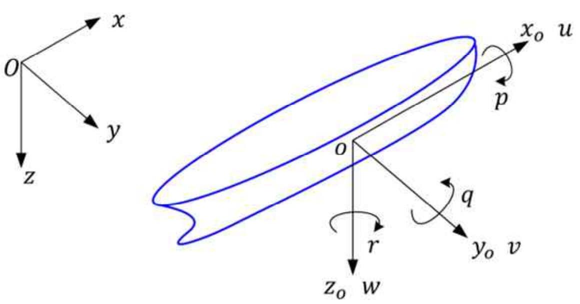

Fig. 8 Coordinate systems

3.2 Model structures

Maneuvering motions are generated by changes in outboard motor angle. So, the rudder forces and moments which are generally applied to assess the maneuvering motions of a commercial ship are not considered as external force and moment. The subscripts E, H, S and T indicate external, hydrodynamic, hydrostatic and thrust, respectively.

$$\underline{F}_E = \underline{F}_H + \underline{F}_S + \underline{F}_T \tag{3}$$

The hydrodynamic and hydrostatic force and moment are modeled in Eqs. (4)~(5). The coefficients with an overline and tilde written in Eqs. (4)~(5) were estimated by analyzing straight running tests and turning tests, respectively. Hydrodynamic forces and moments consist of added mass and damping forces and moments.

$$\begin{aligned}
X_H &= \overline{X_{\dot{u}}}\dot{u} + \overline{X_{u|u|}}u|u| + \widetilde{X_{vv}}v^2 + \widetilde{X_{rr}}r^2 + \widetilde{X_{vr}}vr \\
Y_H &= \widetilde{Y_{\dot{v}}}\dot{v} + \widetilde{Y_{\dot{p}}}\dot{p} + \widetilde{Y_{\dot{r}}}\dot{r} + \widetilde{Y_v}v + \widetilde{Y_p}p + \widetilde{Y_r}r \\
&\quad + \widetilde{Y_{v|v|}}v|v| + \widetilde{Y_{r|r|}}r|r| + \widetilde{Y_\phi}\phi \\
Z_H &= \overline{Z_{\dot{w}}}\dot{w} + \overline{Z_{\dot{q}}}\dot{q} + \overline{Z_0} + \overline{Z_w}w + \overline{Z_q}q \\
K_H &= \widetilde{K_{\dot{v}}}\dot{v} + \widetilde{K_{\dot{p}}}\dot{p} + \widetilde{K_{\dot{r}}}\dot{r} + \widetilde{K_v}v + \widetilde{K_p}p + \widetilde{K_r}r + \widetilde{K_{r|r|}}r|r| \\
M_H &= \overline{M_{\dot{w}}}\dot{w} + \overline{M_{\dot{q}}}\dot{q} + \overline{M_0} + \overline{M_w}w + \overline{M_q}q \\
&\quad + \overline{M_{w|w|}}w|w| + \overline{M_{q|q|}}q|q| + \widetilde{M_{|r|}}|r| + \overline{M_z}z \\
N_H &= \widetilde{N_{\dot{v}}}\dot{v} + \widetilde{N_{\dot{p}}}\dot{p} + \widetilde{N_{\dot{r}}}\dot{r} + \widetilde{N_v}v + \widetilde{N_p}p + \widetilde{N_r}r \\
&\quad + \widetilde{N_{v|v|}}v|v| + \widetilde{N_{r|r|}}r|r| + \widetilde{N_\phi}\phi
\end{aligned} \tag{4}$$

$$\begin{aligned}
X_S &= 0 \\
Y_S &= 0 \\
Z_S &= \overline{Z_z}z \\
K_S &= \widetilde{K_\phi}\phi \\
M_S &= \overline{M_\theta}\theta \\
N_S &= 0
\end{aligned} \tag{5}$$

3.3 Model parameters

The model parameters, written on the right hand sides of Eqs. (4)~(5), were obtained with trial and error methods based on specific characteristics of each hydrodynamic coefficient. In order to effectively tune the mathematical models and obtain those hydrodynamic coefficients, it was important to clearly identify the meaning of the

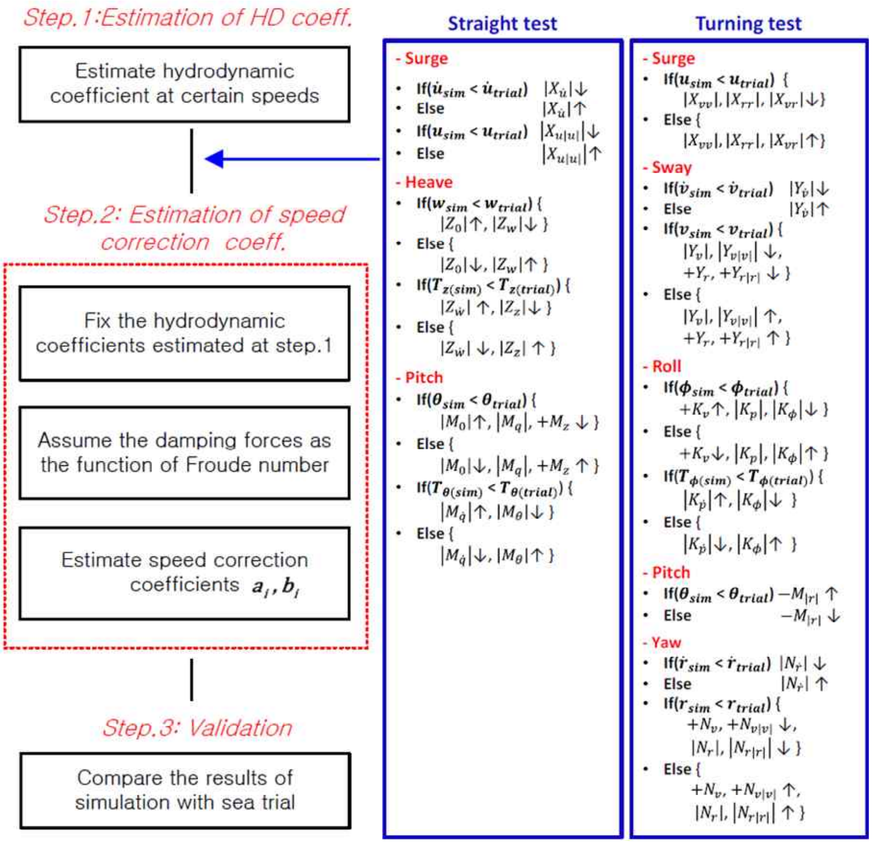

Fig. 9 Simple trial and error method used to find model parameters

hydrodynamic coefficients.

The trial and error method used to find the model parameters of hydrodynamic force is shown in Fig. 9. The 1st step in finding a model parameter is to estimate the hydrodynamic and hydrostatic coefficients, which are included in Eqs. (4)~(5). In order to find those coefficients, the results of the sea trial listed in Table 3 were used. Correction for motion variables of surge, heave, and pitch in the time domain was possible with the simple IF-THEN-ELSE tuning method.

When tuning surge, sway, and heave coefficients in straight running tests, the important coefficients are $X_{u|u|}$, Z_0, Z_z, M_0, M_z and M_θ. Z_0 and M_0 indicate the lift and moment. In the case of the turning test, surge velocity should be reduced when sway velocity and yaw angular velocity are increased. The surge hydrodynamic coefficients influenced by sway and yaw are X_{vv}, X_{rr} and X_{vr}. Especially, the added mass coefficient X_{vr} is the most sensitive coefficient, indicating the surge, sway, and yaw coupling effect. When considering the coupled effects sway, yaw and roll, while the ship is turning, are very important because of the coupled hydrodynamic coefficients Y_r, $Y_{r|r|}$, N_v, $N_{v|v|}$, K_v and K_r. So, the motion variables of sway, yaw, and roll differ depending on one another when tuning horizontal motion. The coefficients involved in turning are $Y_{v|v|}$, N_r, K_v, K_p and K_ϕ. In the case of a commercial ship, the most important stability coefficient is generally a negative value. However, N_v of a planning hull becomes a positive value owing to stern dominancy. In order for a simulator to be stable, it is better for N_v to be a positive value.

K_v is also an important coefficient for the stability of a simulator. If K_v appears to be a large positive value, roll angle increases because it adversely affects decay roll motion. So, it is recommended that K_v has a small positive value for stability and inward roll motion during turning.

Regarding step 2 in Fig. 9, we assumed that the changes in hydrodynamic damping force and moment are quadratic functions with respect to Froude number. The reason why this assumption only applies to the damping forces and moments is because of the simplification of the mathematical models and the calculation time.

If the hydrodynamic and hydrostatic coefficients are obtained at a certain Froude number, those coefficients should then be fixed. That way, the effects of the changes in ship speed can be adjusted by correcting coefficients a and b in Eq. (6). The speed correction coefficients a and b are obtained by repetitive tuning after confirming with the results of sea trials. If a and b are zero, hydrodynamic forces and moments are not changed by speed. Mathematically, damping force and moment increase as a and b increase if Fn/Fn_0 is less than one. It is advisable to adjust b when the effects of speed changes are strong.

$$\underline{F}_D(Fn) = \underline{F}_D\left\{1 + a_i(1 - Fn/Fn_0) + b_i(1 - Fn/Fn_0)^2\right\},\quad i = 1, \ldots, 6 \tag{6}$$

where,

$\underline{F}_D(Fn)$	Damping force vector reflecting speed change
$\underline{F}_D$	Damping force vector at nominal Froude number
a_i	1st order coefficient of the quadratic function
b_i	2nd order coefficient of the quadratic function
Fn	Froude number
Fn_0	Nominal Froude number at step. 1 in Fig. 9

Table 4 Nondimensional hydrodynamic and hydrostatic coefficients at Froude number 0.83

Surge		Sway		Heave	
$X_{\dot{u}}'$	-6.50E-3	$Y_{\dot{v}}'$	-3.88E-2	$Z_{\dot{w}}'$	-3.88E-2
$X_{u\|u\|}'$	-1.20E-2	$Y_{\dot{p}}'$	0.00E+0	$Z_{\dot{q}}'$	0.00E+0
X_{vv}'	-4.80E-4	$Y_{\dot{r}}'$	0.00E+0	Z_0'	-1.00E-4
X_{rr}'	-3.80E-4	Y_v'	-1.05E-2	Z_w'	-1.00E-1
X_{vr}'	-3.10E-2	Y_p'	0.00E+0	Z_q'	-5.00E-2
		Y_r'	9.00E-4	Z_z'	-1.00E+0
		$Y_{v\|v\|}'$	-8.80E-2		
		$Y_{r\|r\|}'$	1.00E-5		
		Y_ϕ'	0.00E+0		
Roll		**Pitch**		**Yaw**	
$K_{\dot{v}}'$	0.00E+0	$M_{\dot{w}}'$	0.00E+0	$N_{\dot{v}}'$	0.00E+0
$K_{\dot{p}}'$	-5.56E-4	$M_{\dot{q}}'$	-2.42E-3	$N_{\dot{p}}'$	0.00E+0
$K_{\dot{r}}'$	0.00E+0	M_0'	2.00E-1	$N_{\dot{r}}'$	-9.22E-3
K_v'	1.06E-2	M_w'	-4.00E-3	N_v'	1.30E-4
K_p'	-1.80E-3	M_q'	-5.00E-1	N_p'	0.00E+0
K_r'	-5.10E-5	$M_{w\|w\|}'$	1.00E-2	N_r'	-4.32E-2
$K_{r\|r\|}'$	0.00E+0	$M_{q\|q\|}'$	0.00E+0	$N_{v\|v\|}'$	0.00E+0
K_ϕ'	-8.95E-3	$M_{\|r\|}'$	-4.00E-1	$N_{r\|r\|}'$	-7.08E-3
		M_z'	7.35E+0	N_ϕ'	-1.00E-4
		M_θ'	-5.00E-1		

Table 5 Tuned speed correction coefficients

Motion	i	Coefficient	
		a_i	b_i
Surge	1	1.05	1.00
Sway	2	1.07	1.20
Heave	3	1.00	1.00
Roll	4	1.32	0.95
Pitch	5	1.12	1.05
Yaw	6	1.12	0.80

4. Simulation and validation

Figs. 10~12 show the results of sea trial and mathematical model. Since real sea condition was not flat and the thrust could not be kept uniform during sea trial test, there are small variation in sea trial results. So, the performance of mathematical model was evaluated by the comparing with the average values of sea trials. The error limit between the results of sea trial test and mathematical model was set to ±10 %.

In straight running tests, as shown in Figs. 10~11, pitch angles according to various surge velocities are confirmed. In order for the simulation to match with the sea trial during the transition interval of surge velocities in the time domain, the added mass coefficient $X_{\dot{u}}$ should be corrected, as in Fig. 9. Since $X_{\dot{u}}$ is very small compared to $Y_{\dot{v}}$, increasing $X_{\dot{u}}$ to match during the transition interval of surge velocities is not effective. The criterion used to evaluate pitch angle in the simulation is the convergence value. As shown in Fig. 11, similar converging tendencies between the simulation and sea trial are seen.

Fig. 12 shows the time history of motion variables in the zig zag test. Contrary to general zig zag tests, which are performed to evaluate yaw-checking ability, such as 10-10 zig zag and 20-20 zig zag, the current scenario is that the thruster deflects fully at an angle of 35° for 5 seconds and then changes in the opposite direction for 5 seconds. As shown in Fig. 12, sway velocity and roll angle in the simulation correspond to that in the sea trial, while surge velocity and yaw rate have some slight differences. So, it is necessary to adjust X_{vv}, X_{rr} and X_{vr} and reduce the yaw hydrodynamic damping moment.

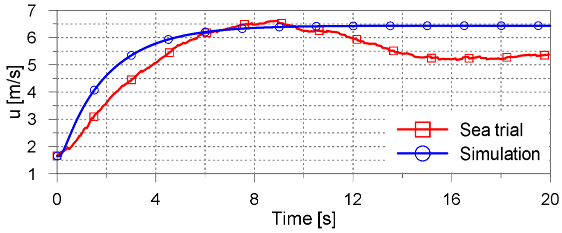

(a) ST01 (Low speed)

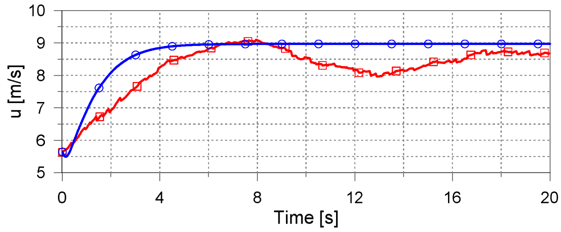

(b) ST02 (Middle speed)

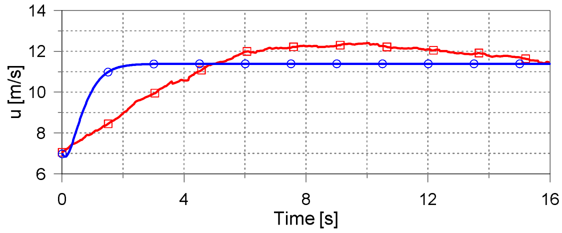

(c) ST03 (High speed)

Fig. 10 Surge velocity in straight running test

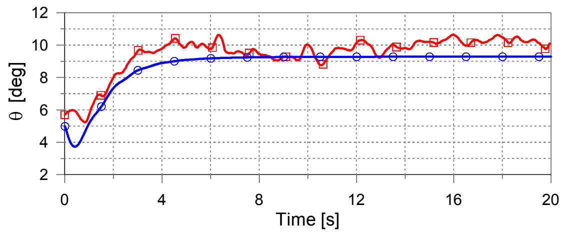

(a) ST01 (Low speed)

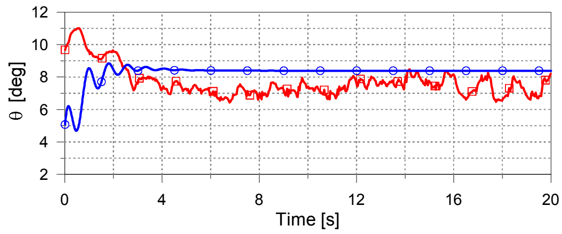

(b) ST02 (Middle speed)

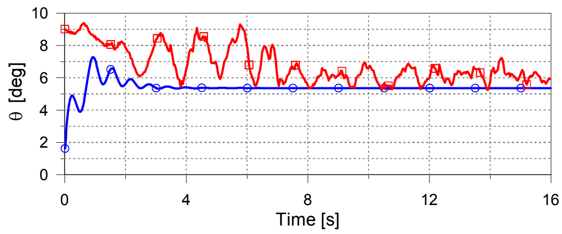

(c) ST03 (High speed)

Fig. 11 Pitch angle in straight running test

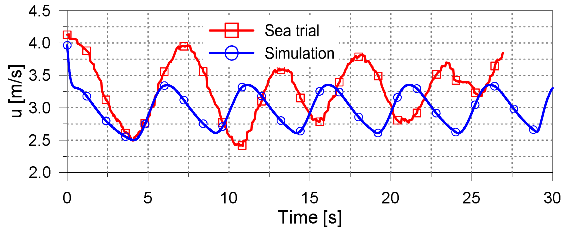

(a) Surge velocity

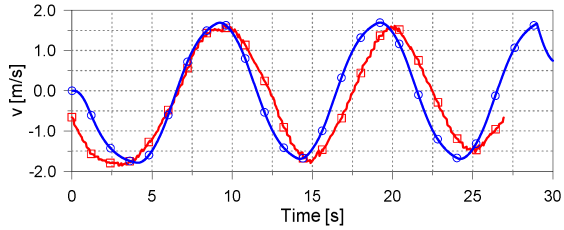

(b) Sway velocity

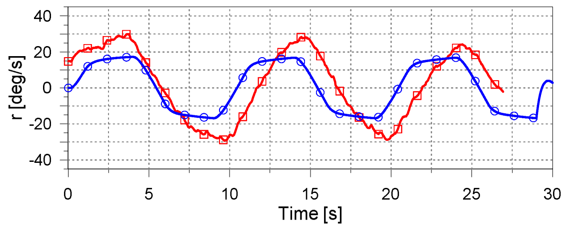

(c) Yaw rate

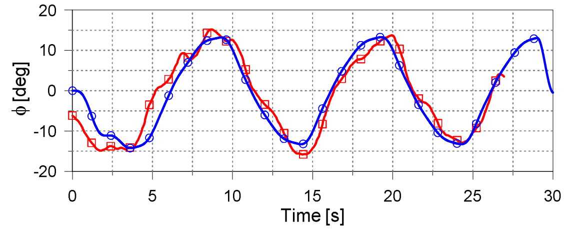

(d) Roll angle

Fig. 12 Comparison of Simulation and Sea trial in the zig zag test (ZZ01)

Figs. 13~14 show the results of the turning simulation and the sea trial. If the speed increases, roll angle also increases in the sea trial. So, this phenomenon should be implemented in the simulation as well. The relevant mathematical parameters are the sway-roll and yaw-roll coupled coefficients K_v and K_r. As in the zig zag test, the yaw rate in the simulation is a little less than the one in the sea trial. Even though the trends of surge, sway, yaw, and roll motion variables are similar between the simulation and the sea trial, the trajectory differs since errors accumulate during numerical integration.

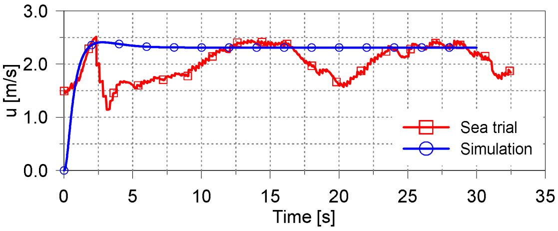

(a) Surge velocity

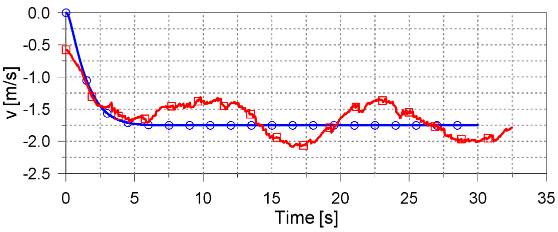

(b) Sway velocity

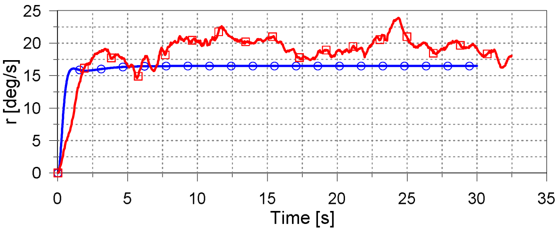

(c) Yaw rate

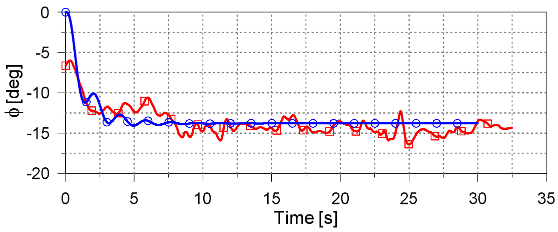

(d) Roll angle

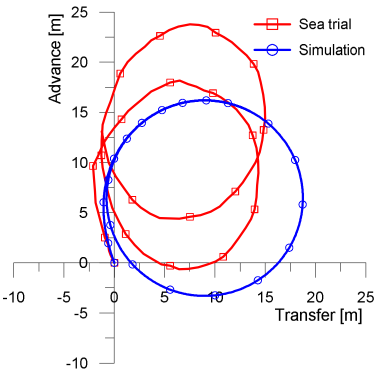

(e) xy trajectory

Fig. 13 Comparison of Simulation and Sea trial in a turning test (TR01)

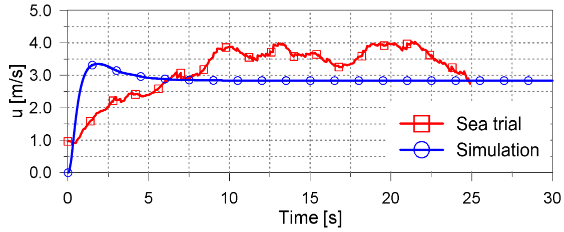

(a) Surge velocity

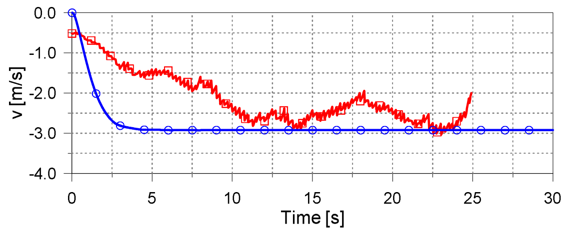

(b) Sway velocity

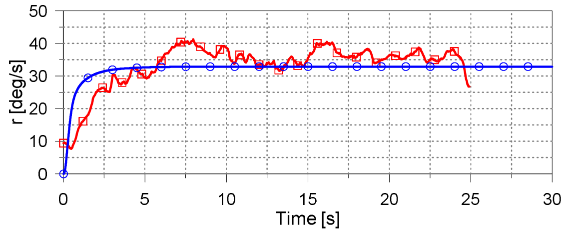

(c) Yaw rate

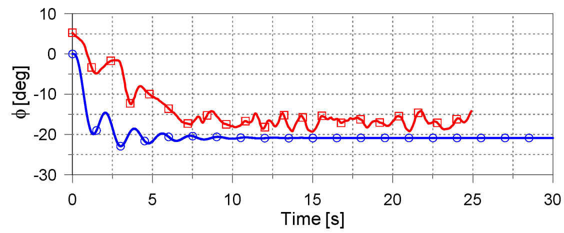

(d) Roll angle

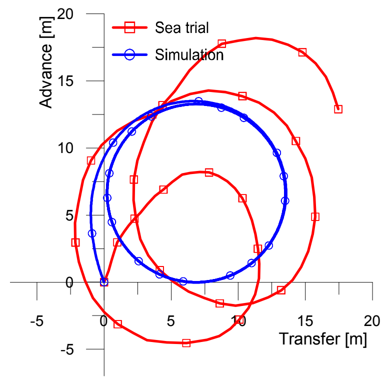

(e) xy trajectory

Fig. 14 Comparison of Simulation and Sea trial in a turning test (TR02)

5. Conclusion

In order to acquire reference data on motion characteristics, a sea trial was carried out. A mathematical model for a ship handling simulator of a motor boat was developed. The model parameters consisting of hydrodynamic and hydrostatic force and moment were obtained by using a trial and error method based on the specific characteristics of hydrodynamic coefficients. Hydrodynamic damping forces and moments are assumed as the quadratic function of Froude number to reflect the effects of speed changes. Finally, the mathematical model was verified by comparing the results of the simulation with those of the sea trial. So, the feasibility of using the mathematical model for a ship handling simulator was confirmed.

Sea trial test of a small boat is affected largely by external disturbance like wind, wave and current. In the future, those environmental effects are also analyzed when the models of hydrodynamic force and moment are estimated.

Acknowledgements

This research is financially supported by Changwon National University in 2015~2016

References

[1] A Promotion Plan for Marina Industry, 2014.

[2] Fossen, T. I.(1994), Guidance and Control of Ocean Vehicles, John Wiley & Son.

[3] Kang, N. S. and Yoon, H. K.(2013), "A Study for the Conceptual Design of a Small Leisure Boat Handling Simulator", Journal of the Korea Society for Simulation, Vol. 22, No. 4, pp. 99-107.

[4] Kim, D. J., Yeo, D. J. and Rhee, K. P.(2010), "Development of a Simple Manoeuvring Model for Ship-handling Simulator by Analytical Methods", Journal of the Society of Naval Architects of Korea, Vol. 47, No. 6, pp. 776-781.

[5] Lewandowski, E. M.(2002), The Dynamics of Marine Craft, World Scientific.

[6] Yeo, D. J. and Rhee, K. P.(2005), "A Study on the Sensitivity Analysis of Submersibles' Manoeuvrability", Journal of the Society of Naval Architects of Korea, Vol. 42, No. 5, pp. 458-465.

[7] Yoon, H. K. and Kang, N.(2016), "Modeling and Simulation of the 6 DOF Motion of High Speed Planing Hull Running in Calm sea", Journal of the Society of Naval Architects of Korea, Vol. 53, No. 1, pp. 10-17.

[8] Yoon, H. K., Yeo, D. J., Fang, T. H., Yoon, K. H., and Lee, C. M.(2007a), "A Simplified Horizontal Maneuvering Model of a RIB-Type Target Ship", Journal of the Society of Naval Architects of Korea, Vol. 44, No. 6, pp. 572-578.

[9] Yoon, H. K., Son, N. S. and Lee, G. J.(2007b), "Estimation of the Roll Hydrodynamic Moment Model of a Ship by Using the System Identification Method and the Free Running Model Test, IEEE Journal of Oceanic Engineering, Vol. 32, No. 4, pp. 798-806.

[10] MEMSIC company website: http://www.memsic.com/inertial-systems/

Received 29 August 2016
Revised 17 October 2016
Accepted 17 October 2016